Preclinical Development

Molecular Cancer Therapeutics

In Vitro and *In Vivo* Responses of Advanced Prostate Tumors to PSMA ADC, an Auristatin-Conjugated Antibody to Prostate-Specific Membrane Antigen

Xinning Wang[1], Dangshe Ma[2], William C. Olson[2], and Warren D.W. Heston[1]

Abstract

Prostate-specific membrane antigen (PSMA) is a membrane protein that is overexpressed manifold in prostate cancer and provides an attractive target for therapy. PSMA ADC is an antibody-drug conjugate (ADC) that consists of a fully human anti-PSMA monoclonal antibody conjugated to monomethylauristatin E through a valine-citrulline linker. In this study, the antitumor activity of PSMA ADC was evaluated against a panel of prostate cancer cell lines *in vitro* and in a novel *in vivo* model of taxane-refractory human prostate cancer. *In vitro* cell killing was efficient for cells with abundant PSMA expression (>10^5 molecules/cell; $IC_{50} \leq$ 0.022 nmol/L) and 1,000-fold less efficient for cells with undetectable PSMA (IC_{50} > 30 nmol/L). Intermediate potency (IC_{50} = 0.80 nmol/L) was observed for cells with approximately 10^4 molecules of PSMA per cell, indicating a threshold PSMA level for selective cell killing. Similar *in vitro* activity was observed against androgen-dependent and -independent cells that had abundant PSMA expression. *In vitro* activity of PSMA ADC was also dependent on internalization and proper *N*-glycosylation/folding of PSMA. In contrast, less potent and nonselective cytotoxic activity was observed for a control ADC, free monomethylauristatin E, and other microtubule inhibitors. PSMA ADC showed high *in vivo* activity in treating xenograft tumors that had progressed following an initial course of docetaxel therapy, including tumors that were large (>700 mm^3) before treatment with PSMA ADC. This study defines determinants of antitumor activity of a novel ADC. The findings here support the clinical evaluation of this agent in advanced prostate cancer. *Mol Cancer Ther; 10(9); 1728–39. ©2011 AACR.*

Introduction

Prostate cancer is the most common nonskin cancer in men in most Western populations and it kills more than 200,000 men annually worldwide (1). Although conventional treatments, such as surgery, radiation, and androgen suppression, are effective, many patients experience disease recurrence and ultimately succumb to their disease. Hormone-refractory prostate cancer is particularly difficult to control and many treatment protocols include a chemotherapeutic agent. An important consideration is the limited and transient response of prostate cancer to systemic chemotherapy and its potential toxicity. There is an urgent need for additional therapies.

Chemoresistance mechanisms are poorly defined in prostate cancer (2, 3). Docetaxel resistance has been generated *in vitro* (4–8); however, resistance pathways vary depending on the cell line and selection conditions. In addition, clinical resistance to taxanes has been linked to changes in tumor microenvironment and tumor cells (3). Additional preclinical models are needed to better assess the potential utility of new agents against prostate tumors that are refractory to standard therapies.

Monoclonal antibody (mAb) therapy for oncology has grown tremendously in the past decade (9–12). Currently, 7 unconjugated mAbs and 2 radiolabeled mAbs are approved for cancer treatment in the United States with many more in development. However, mAbs to many tumor-associated antigens show limited activity in unmodified form. In such cases, mAbs can be covalently linked to a cytotoxic drug as a potential means to selectively deliver the drug to neoplastic cells while reducing toxicity toward healthy tissues. Antibody-drug conjugates (ADC) hold increasing promise due to continuing advances in cancer proteomics, antibody engineering, and drug-linker chemistries (9, 10, 13–15). Newer ADCs have shown substantial clinical activity as single agents even in heavily pretreated patients (11, 16).

Authors' Affiliations: [1]Department of Cancer Biology, Cleveland Clinic Foundation, Cleveland, Ohio; and [2]Progenics Pharmaceuticals, Inc., Tarrytown, New York

Note: Supplementary data for this article are available at Molecular Cancer Therapeutics Online (http://mct.aacrjournals.org/).

Current address for D. Ma: Pfizer Inc., 401 North Middletown Road, Pearl River, NY 10965.

Corresponding Author: Warren D.W. Heston, Cleveland Clinic, 9500 Euclid Ave., Cleveland, OH 44195. Phone: 216-444-8181; Fax: 216-445-0610; E-mail: hestonw@ccf.org

doi: 10.1158/1535-7163.MCT-11-0191

Prostate-specific membrane antigen (PSMA) is an attractive target for the treatment and detection of prostate cancer. It is a type II transmembrane protein with a short intracellular domain (amino acids 1–18), a transmembrane domain (amino acids 19–43), and a large extracellular domain (amino acids 44–750; refs. 17–19). PSMA is expressed in nearly all prostate cancers, and expression is highest in poorly differentiated, metastatic, and hormone-refractory cases (17, 20–22). PSMA also is expressed in a variety of tumors, but not normal, vascular endothelium, which further broadens its potential utility as a therapeutic target (23–25). The cytoplasmic tail of PSMA mediates its internalization both in the presence and absence of mAbs (26, 27). With its abundant and restricted expression in tumors, its membrane location, and rapid internalization, PSMA has characteristics desired in a target for ADC therapy.

Monomethylauristatin E (MMAE) is a synthetic dolastatin 10 analogue that potently blocks tubulin polymerization. Dose-limiting toxicities of neutropenia, myalgia, and constipation have been reported for dolastatin 10 (28, 29), and drugs in this class may be more useful when selectively directed to cancer cells. An example of such targeted drug delivery is provided by brentuximab vedotin (SGN-35), an anti-CD30 mAb conjugated to MMAE through a valine-citrulline (vc) dipeptide linker. Brentuximab vedotin has shown promising tolerability and activity in the treatment of relapsed or refractory Hodgkin lymphoma and systemic anaplastic large-cell lymphoma (11, 30).

PSMA ADC (Fig. 1) comprises a fully human anti-PSMA mAb conjugated to vcMMAE (31). PSMA ADC is designed to selectively bind PSMA-expressing cells, internalize via the endocytic pathway, and release a cytotoxic dose of MMAE. The agent has entered phase 1 testing in patients with metastatic prostate cancer that has progressed following androgen deprivation and taxane therapy. In the ongoing study, antitumor activity has been observed as decreases in prostate-specific antigen, circulating tumor cells, and/or bone pain at generally well-tolerated doses (32).

To further elaborate the antitumor spectrum of this agent, we report here the *in vitro* activity of PSMA ADC against androgen-dependent and -independent prostate cancer cell lines with varying levels of PSMA expression. We also describe the efficacy of PSMA ADC in a novel *in vivo* model of docetaxel-refractory prostate cancer. Overall, our findings provide insight into the potential utility of this targeted therapy in advanced prostate cancer.

Materials and Methods

Cell culture

Prostate cancer cell lines were obtained from American Type Culture Collection (ATCC). LNCaP, C4-2, CWR22rv1, and PC3 cells were maintained in RPMI1640 (Mediatech Inc.) supplemented with 2 mmol/L L-glutamine and 10% FBS (United States Biochemicals). DU145 cells were maintained in Dulbecco's Modified Eagle's Medium (Mediatech Inc.) supplemented with 2 mmol/L L-glutamine and 10% FBS (United States Biochemicals). MDA PCa2b cells were grown in F-12K Medium (ATCC) supplemented with 20% FBS, 25 ng/mL cholera toxin, 10 ng/mL mouse epidermal growth factor, 0.005 mmol/L phosphoethanolamine, 100 pg/mL hydrocortisone, 45 nmol/L selenious acid, and 0.005 mg/mL bovine insulin.

Cytotoxic agents and antibodies

Paclitaxel and docetaxel were purchased from Sigma-Aldrich. PSMA ADC, control ADC (human IgG conjugated to vcMMAE), and MMAE were prepared as described (31). Anti-PSMA mAbs J591 and GCP.04 were gifts from Dr. Neil Bander (Weill Cornell Medical College, New York) and Dr. Jan Konvalinka (Academy of Sciences, Prague, Czech Republic), respectively.

Transfection of PC3 cells

PSMA point mutants with altered internalization (L5A) and *N*-linked glycosylation (N638A) have been described (33, 34). DNA (5 μg) was precipitated with PIRES-puro (0.5 μg) and transfected into PC3 cells using Lipofectamine 2000 (Invitrogen). Stable clones were selected with 1 μg/mL puromycin.

Extraction of cell membrane

One 175-cm^2 flask of harvested cells was diluted with 10 mL of 50 mmol/L Tris (pH 7.5), Dounce homogenized, and centrifuged at 3,000×*g* at 4°C for 5 minutes. Supernatant was collected and ultracentrifuged at 70,000×*g* at 4°C for 35 minutes. The pellet was then washed and homogenized in Tris buffer. Protein concentration was measured by BCA assay (Thermo Scientific).

Western blotting

Cell membrane extract (20 μg protein) was resolved by 7.5% bis-acrylamide reducing SDS-PAGE and transferred to nitrocellulose. Membranes were blocked with 5% milk in Tris Buffered Saline-Tween 20 (TBST) for 1 hour at room temperature. PSMA was detected with mAb J591 or GCP.04 at approximately 0.2 μg/mL for 1 hour followed by incubation with horseradish peroxidase-goat–anti-mouse IgG antibody (1:5,000 dilution) for 1 hour. After 3 TBST washes, blots were visualized by chemiluminescence.

Folate hydrolase assay

Cell membrane extract (2 μg) was combined with 5 nmol of methotrexate diglutamate ($MTXGlu_2$; Schircks Laboratories). The reaction mixture was adjusted to 100 μL with 50 mmol/L Tris (pH 7.5), incubated at 37°C for 1 hour, and stopped with 100 μL 0.5 mol/L Na_2HPO_4. Reaction products were quantified by reversed phase high-performance liquid chromatography (33).

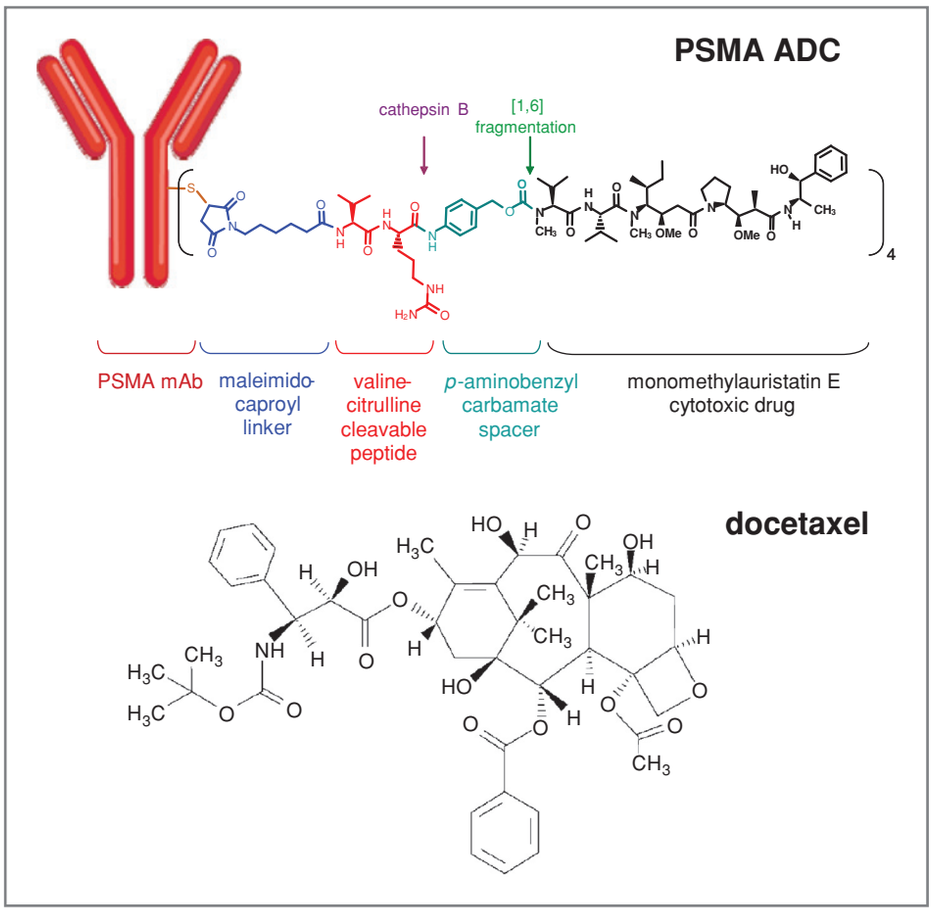

Figure 1. Structures of PSMA ADC and docetaxel.

Binding of cell lines to *N*-[*N*-[(*S*)-1,3-dicarboxypropyl]carbamoyl]-*S*-[^{3}H]-methyl-L-cysteine

Cells (5×10^5) were incubated with *N*-[*N*-[(*S*)-1,3-dicarboxypropyl]carbamoyl]-*S*-[^{3}H]-methyl-L-cysteine (^{3}H-ZJ24; GE Healthcare Life Sciences) in a total volume of 200 μL of 50 mmol/L Tris (pH 7.5) for 1 hour at 37°C. The mixture was centrifuged at 3,000×*g* for 5 minutes at 4°C to separate bound and free ^{3}H-ZJ24. The supernatant was removed, and the cell pellet was washed 3 times with 500 μL of cold Tris buffer. Four milliliters of ECOLUME scintillation cocktail (MP Biomedicals) was added, and radioactivity was counted. Nonspecific binding was determined using the same method in the presence of 0.1 mmol/L phosphonomethyl pentanedioic acid. Data were analyzed using GraphPad Prism 3.0.

In vitro cytotoxicity assay

Cytotoxicity was measured by using the CellTiter 96 Aqueous Cell Proliferation Assay (Promega). Briefly, cells (3,000/well) were seeded in 96-well culture plates the day before treatment and then incubated with drugs for 72 hours. Colorimetric reagent was then added to each well. After a 3-hour incubation at 37°C, the absorbance at 490 nm was measured, and IC_{50} was determined by GraphPad Prism. Where indicated, assays were done in the presence of 1 μg/mL of J591 or 10 μmol/L of ZJ24 (Bachem Inc.) to assess the effect on the activity of PSMA ADC.

Generation of docetaxel-refractory xenograft tumors

Male athymic nude mice (6 to 8 weeks old, Charles River Laboratories) were each implanted with 5 million C4-2 cells in Matrigel (Becton Dickinson) by subcutaneous injection into the right flank. Fourteen days later, animals with tumor volumes between 100 mm^3 and 200 mm^3 were randomized to receive 2 mg/kg docetaxel ($n = 50$) or vehicle ($n = 10$) by weekly injection via the tail vein. This dose represents the maximum tolerated dose in this model (data not shown). Docetaxel was administered in PBS containing 0.6% ethanol and 1.5% polysorbate 80. Tumor volume, body weight, physical appearance, and survival were recorded twice weekly. Tumor volume was calculated as (length) × (width^2)/2.

Treatment of docetaxel-refractory xenograft tumors

When the tumor volume of a docetaxel-treated animal exceeded 400 mm^3, the animal was rerandomized 1:1 to receive weekly IV treatment with either 6 mg/kg PSMA ADC or 2 mg/kg docetaxel. Animals were monitored twice weekly and euthanized when in distress or when tumor volume exceeded 2,000 mm^3. The study was terminated 182 days after tumors were implanted. The study was conducted in accordance with Institutional Animal Care and Use Committee guidelines.

Statistical analyses

Intergroup differences in tumor volume and body weight were evaluated for significance via *t* tests. Differences in survival and categorical variables were assessed using log-rank tests and Fisher's exact tests, respectively. Results from 2-tailed tests are reported. Statistical analyses were done using GraphPad Prism.

Results

PSMA expression in prostate cancer cells

PSMA expression was first examined by Western blotting. PSMA was highest in MDA PCa2b cells followed by LNCaP cells, C4-2 cells, and CWR22rv1 cells (Fig. 2A). PC3 cells and DU145 cells had no detectable expression of PSMA.

PSMA has carboxypeptidase activity, and its substrates include polyglutamated folates (35, 36). Folate hydrolase activity correlated well with PSMA expression observed by Western blotting (Fig. 2B). Cells with higher expression of PSMA exhibited higher enzymatic activity. No enzymatic activity was observed in cells that were PSMA-negative by Western blotting.

PSMA expression was further characterized using ZJ24, a urea-based inhibitor of PSMA's enzymatic activity (37). Binding results were fitted to a 1-site binding model (Supplementary Fig. S1). Specific binding was observed only in PSMA-positive cells with K_D values between 35.6 to 46.5 nmol/L (Table 1). The maximum binding capacities (B_{max}) to PSMA-positive cells ranged from 26,600 to 319,000 molecules of ZJ24 per cell. The highest B_{max} was observed in MDA PCA2b cells, which had the highest expression of PSMA by Western blotting. Next highest were LNCaP cells with B_{max} of 251,900 molecules/cell, C4-2 cells with 204,900 molecules/cell, and CWR22rv1 with 26,600 molecules/cell. PSMA is a symmetric dimer that contains 2 identical binding sites for ZJ24 (18, 38); therefore, expression of dimeric PSMA was estimated to range from 13,300 to 159,500 molecules/cell.

Cytotoxicity of PSMA ADC and control inhibitors toward prostate cancer cell lines

Human prostate cancer cell lines were examined for susceptibility to killing by PSMA ADC, free MMAE, unconjugated PSMA mAb, and a control ADC of irrelevant specificity. The activity of PSMA ADC was highly dependent on PSMA expression, with IC_{50} approximately 20 pmol/L for cells with more than 10^5 molecules/cell, IC_{50} = 804 pmol/L for CWR22rv1 cells with 10^4 molecules/cell and IC_{50} > 30,000 pmol/L for PSMA-negative cells (Fig. 2C, Table 1). The control ADC showed weak activity (IC_{50} > 50,000 pmol/L) that was independent of PSMA expression (Fig. 2C, Table 1). Unconjugated PSMA mAb showed no cytotoxicity at concentrations ranging to 1 μmol/L. MMAE had approximately 1,000 pmol/L activity against each of the cell lines.

Docetaxel and paclitaxel are mitotic inhibitors whose mechanism of action resides in stabilizing microtubules in contrast with destabilizers such as MMAE (39). Docetaxel and paclitaxel were active against each of the prostate cancer cell lines, with IC_{50} values of 1.2 to 7.5 nmol/L and 5.9 to 46 nmol/L, respectively (Fig. 2C, Table 1). The taxols were modestly more effective against MDAPCa2b, LNCaP, and C4-2 relative to PC3 and DU145.

The *in vitro* potency of PSMA ADC was unaffected by the presence of 10 μmol/L ZJ24, with respective IC_{50} values of 22 ± 14 pmol/L and 29 ± 18 pmol/L observed in the presence and absence of ZJ24 (Fig. 2D). In the presence of 1 μg/mL of anti-PSMA mAb J591, the potency of PSMA ADC was reduced approximately 3-fold (IC_{50} = 106 ± 32 pmol/L).

Cytotoxicity of PSMA ADC to PC3 cells transfected with wild-type or mutant PSMA

To further investigate the determinants of PSMA ADC's activity, PC3 cells were engineered to express wild-type PSMA (PC3wtPSMA), glycosylation mutant PSMA (PC3N638A), internalization mutant PSMA (PC3L5A), or vector control (PC3PIRESpuro). Transfectants were examined for PSMA expression, folate hydrolase activity, and for ^{3}H-ZJ24 binding. Similar levels of wild type and mutant forms of PSMA ADC were detected by Western blotting (Fig. 3A). Cells that expressed wild-type or internalization mutant PSMA exhibited folate hydrolase activity (Fig. 3B) and specific binding of ^{3}H-ZJ24 (Supplementary Fig. S2 and Table 1), whereas cells that expressed glycosylation mutant PSMA and vector-control cells did not exhibit either property.

PSMA ADC potently killed PC3wtPSMA cells (IC_{50} = 22 pmol/L) but not PC3PIRESpuro cells (IC_{50} > 30,000 pmol/L). PSMA ADC showed minimal activity toward cells that expressed either the internalization mutant (IC_{50} = 8,170 pmol/L) or the glycosylation mutant (IC_{50} = 12,400 pmol/L). The glycosylation mutant adopts a nonnative conformation (33, 34) and does not efficiently bind PSMA ADC (data not shown). The control ADC and PSMA mAb showed weak activity ($IC_{50} \geq$ 30,000 pmol/L) and unmeasurable activity (IC_{50} > 1 μmol/L), respectively, against each of the transfectants. MMAE killed each of the transfected cells with IC_{50} of 594 to 775 pmol/L (Fig. 3C and Table 1).

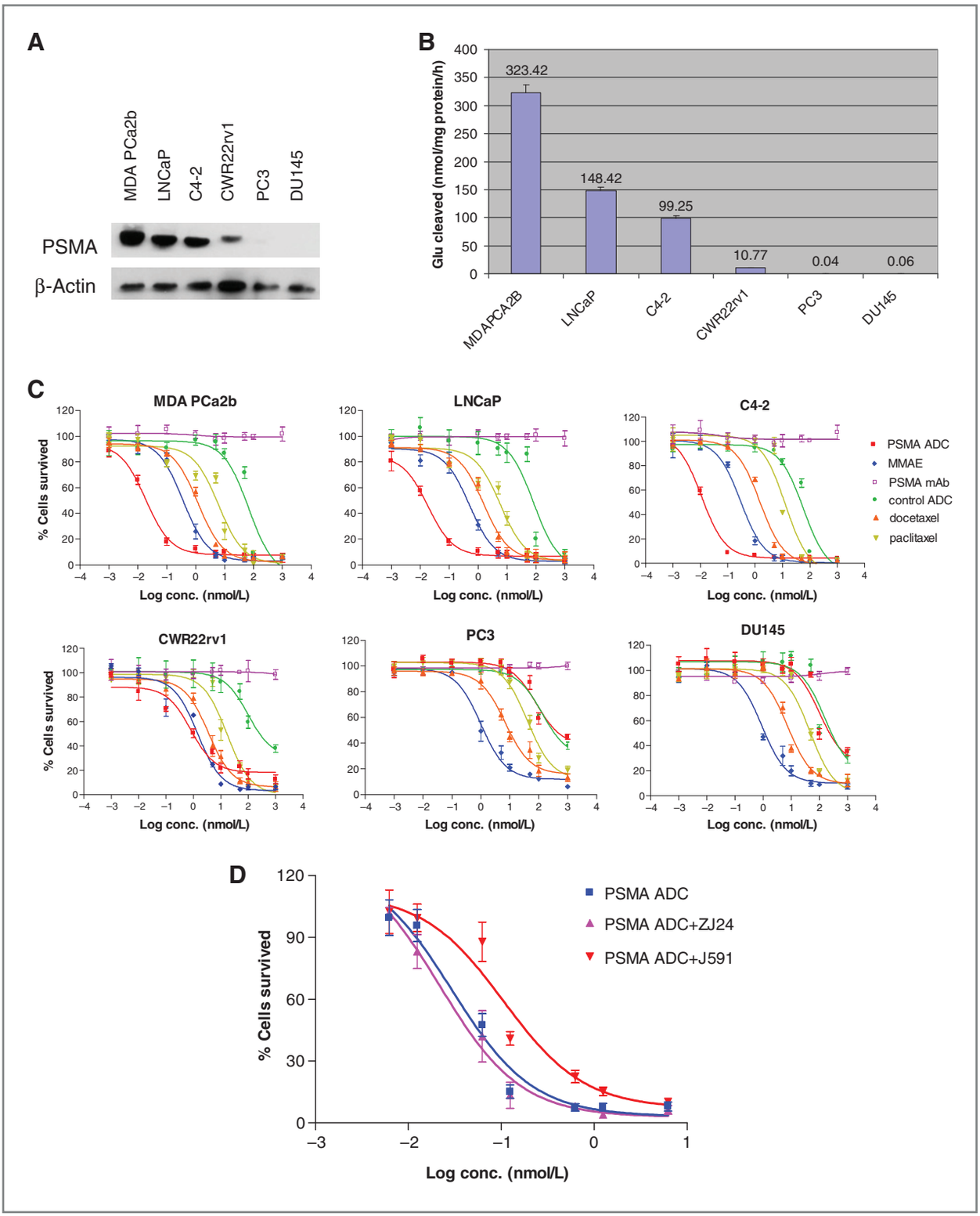

Figure 2. Cytotoxicity of PSMA ADC *in vitro*. A, Western blot analysis of PSMA in lysates from prostate cancer cells. PSMA was detected by J591. B, folate hydrolase assay. Cell membrane (2 μg) was incubated with 5 nmol of $MTXGlu_2$ for 1 hour. MTX formed was determined by high-performance liquid chromatography. Data represent the mean ± SD of triplicate determinations. C, *in vitro* cytotoxicity. Cells were treated for 72 hours with varying concentrations of inhibitor and assessed for viability. D, effect of ZJ24 or J591 on the cytotoxicity of PSMA ADC. C4-2 cells were treated for 72 hours with varying concentrations of PSMA ADC in the presence or absence of 10 μmol/L ZJ24 or 1 μg/mL J591 antibody.

Table 1. PSMA expression and cytotoxicity data

Cell line	Phenotype	ZJ24 Binding		No. of PSMA molecules per cell[a]	IC_{50}, nmol/L				
		B_{max}	K_d, nmol/L		PSMA ADC	MMAE	Control ADC	Docetaxel	Paclitaxel
MDAPCa2b	Androgen dependent PSMA positive	319,000 ± 19,300	46.5 ± 5.9	159,500	0.018 ± 0.008	0.363 ± 0.078	82.1 ± 6.3	1.20 ± 0.27	6.17 ± 1.58
LNCaP	Androgen dependent PSMA positive	251,900 ± 9,300	39.4 ± 2.9	125,950	0.019 ± 0.012	0.502 ± 0.093	78.5 ± 6.6	1.55 ± 0.18	5.90 ± 1.13
C4-2	Androgen independent PSMA positive	204,900 ± 4,600	35.5 ± 0.8	102,450	0.011 ± 0.014	0.298 ± 0.075	57.8 ± 1.9	1.75 ± 0.10	12.6 ± 0.58
CWR22rv1	Androgen independent weakly PSMA positive	26,500 ± 500	35.6 ± 3.9	13,250	0.804 ± 0.167	1.44 ± 0.19	98.8 ± 5.4	3.55 ± 0.66	17.1 ± 1.1
PC3	Androgen independent PSMA negative	no specific binding	N/A	N/A	83.4 ± 6.3	0.970 ± 0.174	96.2 ± 2.3	6.98 ± 0.89	41.8 ± 5.6
DU145	Androgen independent PSMA negative	no specific binding	N/A	N/A	99.1 ± 5.4	0.911 ± 0.120	156.0 ± 5.4	7.47 ± 0.48	46.0 ± 7.8
PC3PIRESpuro	PC3 transfection control	no specific binding	N/A	N/A	31.8 ± 3.7	0.775 ± 0.138	29.9 ± 3.7	ND	ND
PC3wtPSMA	PC3 transfected with wild-type PSMA	75,800 ± 1,100	8.20 ± 1.46	37,900	0.022 ± 0.011	0.667 ± 0.150	38.5 ± 3.8	ND	ND
PC3L5A	PC3 transfected with internalization mutant PSMA	20,700 ± 400	5.06 ± 2.63	10,350	8.17 ± 2.7	0.737 ± 0.175	32.4 ± 2.7	ND	ND
PC3N638A	PC3 transfected with glycosylation mutant PSMA	no specific binding	N/A	N/A	12.4 ± 2.2	0.594 ± 0.110	48.2 ± 2.2	ND	ND

NOTE: Data represent the mean ± SD of triplicate determinations. B_{max} = molecules of ZJ24 per cell. PSMA mAb did not exhibit measurable cytotoxicity at concentrations ranging up to 1,000 nmol/L.

Abbreviations: N/A, not applicable; ND, not done.

[a]Expression levels of dimeric PSMA are estimated to be 1-half of the B_{max} observed for ZJ24, because PSMA is a symmetric dimer that contains 2 identical binding sites for ZJ24.

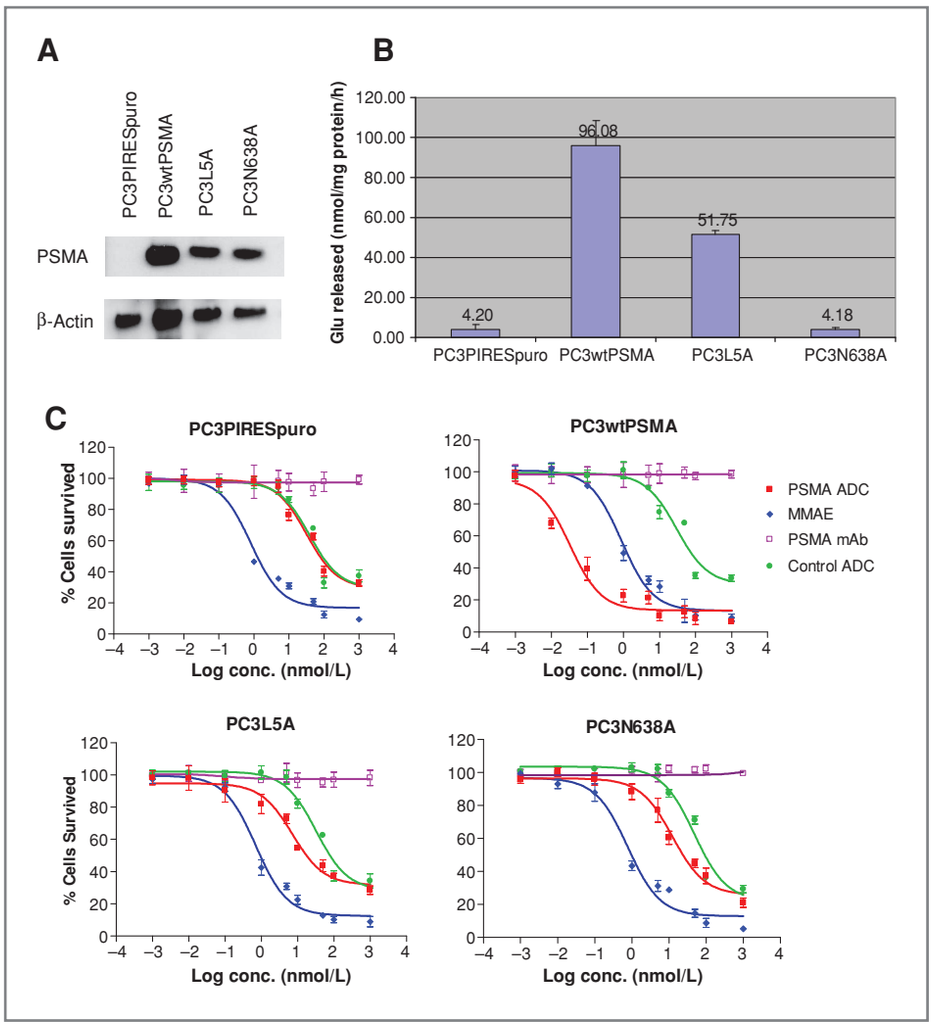

Figure 3. Cytotoxicity of PSMA ADC to transfected PC3 cells. A, Western blot analysis of PSMA in cell lysates. PSMA was detected by GCP.04. B, folate hydrolase assay of cell membrane. Cell membrane (2 μg) was incubated with 5 nmol of $MTXGlu_2$ for 1 hour. MTX formed was determined by high-performance liquid chromatography. Data represent the mean ± SD of triplicate determinations. C, *in vitro* cytotoxicity. PC3 transfectants were treated for 72 hours with inhibitor and then assessed for viability. Data are presented for PC3 cells transfected with empty vector (PC3PIRESpuro), wild-type PSMA (PC3wtPSMA), internalization mutant PSMA (PC3L5A), or glycosylation mutant PSMA (PC3N638A).

Generation of docetaxel-refractory xenograft tumors

A total of 60 animals were included in the xenograft study (Fig. 4A). At 14 days following tumor implantation, animals were randomized to receive docetaxel ($n = 50$) or matched vehicle (group 1, $n = 10$). Of the 50 animals assigned to receive docetaxel, 14 animals had tumors that remained less than 400 mm^3, and these animals continued to receive docetaxel for the duration of the study (group #2). Tumors grew to more than 400 mm^3 in the remaining 36 docetaxel-treated animals, and they were rerandomized 1:1 to receive PSMA ADC (group #3) or to continue docetaxel treatment (group #4). Because the rate of tumor growth varied in individual mice treated with docetaxel, mice were randomized continuously into group #3 or group #4 between days 25 and 119 postimplantation.

The mean tumor volume was 138 mm^3 in both the docetaxel and vehicle groups before initiation of therapy. First-line docetaxel therapy significantly inhibited tumor growth (Fig. 4B). Relative to vehicle-treated animals, docetaxel-treated animals had significantly lower mean tumor volumes ($P \leq 0.03$) at days 21, 25, and 28, as well as a significantly lower rate of progressive tumors more than 400 mm^3 ($P = 0.0014$). Animals in the vehicle group had a median survival of 70 days (range 42–168 days). Median survival in the docetaxel group could not be determined due to rerandomization of progressors. However, 14 docetaxel-treated animals (28%) did not develop tumors more than 400 mm^3 at any time during the study. Of these 14 animals, 3 died of unknown causes, and 11 survived until the end of the study.

Treatment of docetaxel-refractory xenograft tumors

Docetaxel-refractory tumors were defined as those that grew to more than 400 mm^3 in the presence of weekly IV therapy with 2 mg/kg docetaxel. Of the 50 animals that received first-line docetaxel therapy, 36 (72%) developed

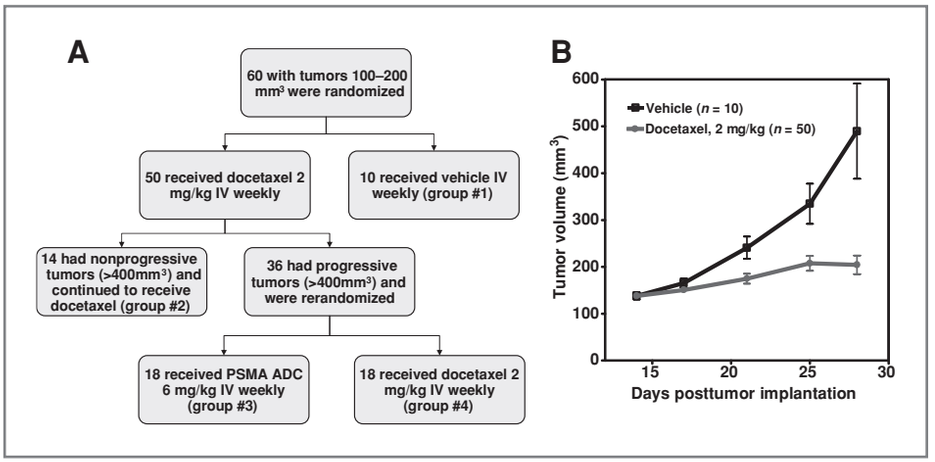

Figure 4. Disposition of study animals and efficacy of first-line therapy with docetaxel. A, disposition of animals among treatment groups. Fourteen days after tumor implantation, animals with 100 to 200 mm^3 tumors were randomized to receive docetaxel (2 mg/kg IV weekly, $n = 50$) or matched vehicle (group #1, $n = 10$). When tumor volume in the docetaxel-treated group exceeded 400 mm^3, the animal was rerandomized 1:1 to receive PSMA ADC (6 mg/kg IV weekly, group #3) or continued docetaxel treatment (2 mg/kg IV weekly, group #4). Mice whose tumors responded durably to docetaxel ($\leq$ 400 mm^3) continued to receive docetaxel at 2 mg/kg IV weekly (group #2). The experiment was terminated 182 days following tumor implantation. B, efficacy of first-line docetaxel therapy. Mean tumor volumes ($\pm$ SEM) of docetaxel- or vehicle-treated animals are plotted up to the time the first docetaxel-treated animals were rerandomized due to tumor progression.

docetaxel-refractory tumors and were rerandomized 1:1 to receive PSMA ADC or continued treatment with docetaxel (Fig. 4A). Mean tumor volumes were 515 $\pm$ 103 mm^3 (range: 410–727 mm^3) and 495 $\pm$ 80 mm^3 (range: 401–650 mm^3) for animals rerandomized to receive PSMA ADC (group #3) or docetaxel (group #4), respectively. The median time of rerandomization was 49 days postimplantation for animals in both group #3 (range 25–119 days) and group #4 (range 25–98 days).

Figure 5 illustrates the change in tumor volumes of the 36 animals that were rerandomized to receive PSMA ADC or continued docetaxel. day 0 represents the time of rerandomization to PSMA ADC or docetaxel. Data before day 0 depict changes in tumor volumes when the animals were on first-line docetaxel therapy.

Tumor volumes decreased in all 18 animals treated with PSMA ADC (Fig. 5A). Rapid regressions were observed even for tumors that were more than 700 mm^3. Although the kinetics of tumor regression varied somewhat (Fig. 5A), 17 of 18 mice (94%) in the PSMA ADC group (group #3) had less than 100 mm^3 tumors at the end of the study. Tumor volume was 166 mm^3 in the remaining group #3 animal. In animals that continued to receive docetaxel, tumors progressed to more than 2,000 mm^3 in all but 2 animals whose tumor volumes were 275 mm^3 and 1,403 mm^3 at the end of the study (Fig. 5B). The difference in the rate of tumor progression between group #3 and group #4 was highly statistically significant ($P < 0.0001$).

Mean tumor volume was significantly lower in the PSMA ADC group relative to the docetaxel group (Fig. 5C; $P \leq 0.0005$) at all time points from 3 to 59 days following rerandomization. Thereafter, few animals remained in the docetaxel group ($n \leq 6$). From an initial value of 515 mm^3 before initiation of PSMA ADC therapy, mean tumor volumes decreased to less than 100 mm^3 within 38 days of treatment and remained less than 100 mm^3 for the duration of the study.

Treatment with PSMA ADC significantly improved survival ($P < 0.0001$, Fig. 5D). At the end of the study, all 18 animals in the PSMA ADC group (group #3) were alive. The median duration of treatment with PSMA ADC was 129 days (range: 87–157 days). In contrast, median survival for group #4 animals was 45 days following rerandomization, and only 2 of 18 animals survived through the end of the study.

PSMA ADC was not associated with any overt toxicity. Physical appearance and activity were unaffected. Mean body weight increased for animals in the PSMA ADC group and decreased for animals in the docetaxel group. The difference in mean body weights of the 2 groups was significant ($P \leq 0.0001$) starting 17 days after rerandomization. The PSMA ADC group had a 20.6% increase in mean body weight 59 days after rerandomization, while the docetaxel group had a 14.5% decrease ($P < 0.0001$). Mean body weight remained stable or increased slightly in the PSMA ADC group thereafter; however, there were too few animals remaining in the docetaxel group for meaningful statistical comparisons.

Discussion

We report *in vitro* and *in vivo* studies of the antitumor activity of PSMA ADC, an anti-PSMA mAb conjugated to vcMMAE. Potent cytotoxicity ($IC_{50} \leq 20$ pmol/L) was observed for androgen-dependent and -independent cells with 10^5 or more molecules of PSMA per cell, and 10^4 molecules per cell served as a threshold level of PSMA

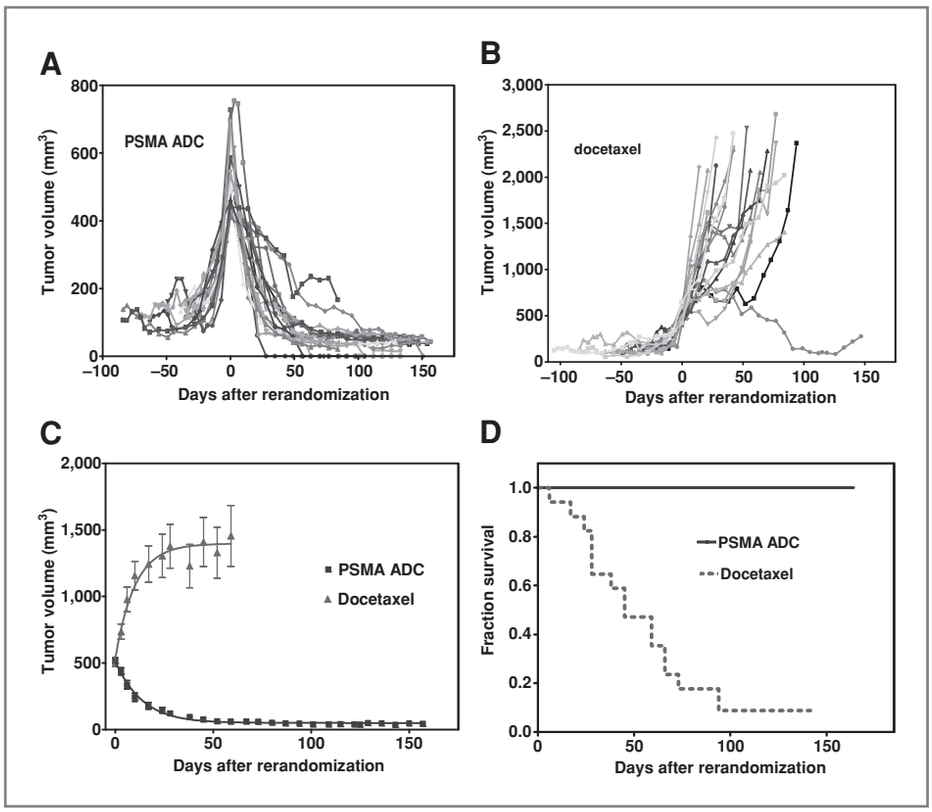

Figure 5. Efficacy of PSMA ADC against docetaxel-refractory tumors. Docetaxel-treated mice with tumors of more than 400 mm^3 were rerandomized 1:1 to receive weekly i.v. treatment with 6 mg/kg PSMA ADC ($n = 18$) or 2 mg/kg docetaxel ($n = 18$). Tumor volumes are shown for individual animals treated with PSMA ADC (A) or docetaxel (B). C, mean tumor volumes (± SEM). Mean tumor volume was significantly lower ($P \leq 0.0005$) in the PSMA ADC treatment group relative to the docetaxel group. D, Kaplan–Meier survival curves. At the end of the study, 18 of 18 animals in the PSMA ADC group and 2 of 18 animals in the docetaxel group were alive ($P < 0.0001$). Median survival for the docetaxel group was 45 days after rerandomization.

expression for selective cytotoxic activity. We also describe the *in vivo* efficacy of this agent in an *in situ* model of taxane-refractory human prostate cancer. PSMA ADC was highly active against tumors that had progressed following an initial course of docetaxel therapy, and even large (>700 mm^3) tumors showed rapid regressions. Our findings establish pharmacologic determinants of activity of a novel ADC. In addition, our *in vivo* model may prove useful for studying second-line therapy with other agents in other tumor settings.

PSMA ADC showed potent and selective activity against PSMA-positive prostate cancer cells. Cells insensitive to PSMA ADC were the PSMA-negative PC3 and DU145 lines, which are poorly differentiated lines. PC3 cells became susceptible to killing by PSMA ADC ($IC_{50} =$ 22 pmol/L) following transfection with PSMA. In contrast to PSMA ADC, a control ADC of irrelevant specificity, free MMAE, and other microtubule inhibitors exhibited less potent *in vitro* activity that was independent of PSMA expression. Unconjugated PSMA mAb did not exhibit intrinsic cytotoxic activity in this study, consistent with prior reports (31, 40, 41); however, our study did not examine the potential for cytotoxic effects mediated by mAb Fc effector functions.

The activity of PSMA ADC was dependent on internalization and proper folding of PSMA, as reduced cytotoxicity was observed against PC3 cells transfected with internalization or *N*-glycosylation mutant forms of PSMA (33, 42). These findings are consistent with PSMA ADC's primary mechanism of action of delivering a potent cytotoxin to the interior of cells that express and internalize native PSMA.

Internalization of PSMA is mediated by a MWNLL motif in its cytoplasmic tail (26). Mutation of this motif did not affect PSMA's enzymatic activity, and the cytotoxicity of PSMA ADC was unaffected by the PSMA inhibitor ZJ24, indicating that internalization and enzymatic activity are unrelated processes. In contrast, mAb J591, which reduces cell-surface levels of PSMA through internalization, reduced the potency of PSMA ADC approximately 3-fold, but complete cell killing was achieved at higher concentrations of PSMA ADC.

Besides being a target for therapy, PSMA has been used to image tumors. Unfortunately, the original imaging agent ^{111}In-capromab pendetide binds an intracellular site on PSMA and has limited utility in imaging bone metastases. Second-generation mAbs to the external domain of PSMA have been found to image bone metastases with nearly 100% accuracy (19). Because imaging would reflect not only site but potentially degree of PSMA expression, imaging tumors before and after therapy could potentially provide a means to assess tumor responses at individual sites. Unlike mAbs, low molecular weight imaging agents do not induce internalization of PSMA and therefore have the potential advantage of not interfering with the antitumor activity of ADCs.

Once prostate cancer becomes refractory to androgen deprivation, chemotherapy with taxanes is indicated; however, the side effects of therapy are appreciable relative to the limited survival benefit. PSMA expression increases following androgen deprivation (22, 43). When tested against androgen-independent C4-2 cells in our study, PSMA ADC was more than 30-fold more potent than docetaxel and paclitaxel. PSMA ADC had minimal activity against PSMA-negative cells, in keeping with the desired reduction in off-target toxicity. PSMA ADC showed selective potency both in androgen-dependent (MDA PCa2b and LNCaP) and androgen-independent (C4-2 and CWR22rv1) PSMA-expressing cell lines, all of which were derived from metastatic disease. The activity of PSMA ADC correlated with PSMA expression in these cells.

Our *in vivo* model reproduces several important features of docetaxel-refractory prostate cancer, including androgen independence, disease progression following an initial response to docetaxel, intersubject variation in rates of progression, and the presence of tumor-stroma interactions. Docetaxel significantly reduced tumor growth ($P = 0.0014$) and prevented disease progression in a substantial fraction of treated animals. By these measures, the efficacy seen in this preclinical model is comparable with docetaxel's clinical efficacy (44). In addition, as seen clinically, most docetaxel-treated tumors eventually progressed and became insensitive to further treatment with docetaxel.

Treatment of docetaxel-refractory tumors with PSMA ADC led to significant improvements in mean tumor volume ($P < 0.0005$) and survival ($P < 0.0001$) relative to continued docetaxel treatment. In addition, mean body weight increased significantly ($P < 0.0001$) in the PSMA ADC group relative to the continued docetaxel group. The 60-animal study, therefore, was sufficiently powered for these endpoints. This approach could potentially be adapted to preclinically assess second-line chemotherapies in other settings.

The efficacy for PSMA ADC observed here is consistent with our prior report, which examined treatment of intramuscular C4-2 tumors (31). In both studies, all tumors responded to treatment with 6 mg/kg PSMA ADC. One important difference between the 2 studies is the duration of treatment. Our prior study used a q4dx6 regimen, and tumors rebounded following cessation of treatment in 3 of 5 animals. This study examined continuous treatment, which resulted in continued tumor suppression. PSMA ADC showed consistent, high-level activity against tumors up to 700 mm^3 in size in the present study and against smaller, disseminated tumors in our previous study. These findings are translationally relevant for prostate cancer, where many patients have micrometastatic tumors that are poorly imaged by conventional radiological methods. Neither unconjugated PSMA mAb nor control ADC showed measurable efficacy against xenografted C4.2 tumors in our prior study (31), indicating that the primary mechanism of antitumor activity in this setting is mAb-mediated delivery of MMAE to PSMA-expressing cells and not nonspecific release of free MMAE or other factors.

The preclinical antitumor activity of PSMA ADC compares favorably with that reported for MLN2704, an ADC comprising humanized J591 linked to drug maytansinoid 1 (40). Against LNCaP cells, the *in vitro* IC_{50} for PSMA ADC (39 pmol/L) is approximately 50-fold less than that reported for MLN2704. In addition, weekly treatment of subcutaneous CWR22 xenografts with 12.9 mg/kg MLN2704 resulted in tumor growth delay but limited tumor regression (40), whereas potent tumor regressions were seen here with 6 mg/kg weekly doses of PSMA ADC. Experimental differences between the 2 studies, however, preclude direct comparison of results.

Several *in vitro* mechanisms of docetaxel resistance have been identified in studies of prostate cancer cells. The mechanisms include tubulin mutations, redistribution of tubulin isoforms, downregulation of thrombospondin-1, loss of PTEN activity, and induction of Stat1 and clusterin (5–8, 45). Less is known regarding clinical resistance. In particular, it remains uncertain whether ATP-binding cassette (ABC) transport proteins play a key role (2). Rather, multifactorial mechanisms have been implicated in clinical resistance to taxanes (2, 3).

The sharp contrast in tumor responses to PSMA ADC or continued docetaxel therapy provides insights into the potential docetaxel resistance pathways operative in this study. Resistance to docetaxel is unlikely to reflect broad upregulation of ABC transporters because both taxanes and MMAE are transported by members of this protein family (46–48); however, we cannot exclude the possibility of selective upregulation of a transporter that confers resistance to docetaxel and not MMAE. Similarly, increased interstitial fluid pressure is unlikely to be a primary cause of resistance, because this mechanism would affect macromolecules to a greater extent than small molecules (49). Docetaxel-refractory tumors maintained PSMA expression at levels sufficient for ADC therapy in this study; this finding is consistent with *in vitro* studies showing that short-term exposure to docetaxel does not affect PSMA expression (50).

This study establishes determinants of PSMA ADC's antitumor activity using a series of primary and engineered prostate cancer cell lines. Selective antitumor activity was observed only in PSMA-expressing cells with more than 10^4 PSMA molecules per cell. Internalization and glycosylation-dependent folding of PSMA were important for the *in vitro* potency of PSMA ADC. In addition, PSMA ADC was broadly and potently active against human prostate tumors that had become refractory to docetaxel treatment *in vivo*. Our findings are relevant to the ongoing clinical investigation of this targeted agent in advanced prostate cancer.

Disclosure of Potential Conflicts of Interest

D. Ma and W. Olson are present or former employees of Progenics Pharmaceuticals and own stock in the company.

Acknowledgments

We thank Haige Zhang for excellent technical assistance.

The costs of publication of this article were defrayed in part by the payment of page charges. This article must therefore be hereby marked *advertisement* in accordance with 18 U.S.C. Section 1734 solely to indicate this fact.

Received March 16, 2011; revised July 6, 2011; accepted July 7, 2011; published OnlineFirst July 12, 2011.

References

1. Jemal A, Siegel R, Xu J, Ward E. Cancer statistics, 2010. CA Cancer J Clin 2010;60:277–300.
2. Mathew P, Dipaola R. Taxane refractory prostate cancer. J Urol 2007;178:S36–41.
3. Seruga B, Ocana A, Tannock IF. Drug resistance in metastatic castration-resistant prostate cancer. Nat Rev Clin Oncol 2011;8:12–23.
4. Kim SJ, Uehara H, Yazici S, Busby JE, Nakamura T, He J, et al. Targeting platelet-derived growth factor receptor on endothelial cells of multidrug-resistant prostate cancer. J Natl Cancer Inst 2006; 98:783–93.
5. Lih CJ, Wei W, Cohen SN. Txr1: a transcriptional regulator of thrombospondin-1 that modulates cellular sensitivity to taxanes. Genes Dev 2006;20:2082–95.
6. Makarovskiy AN, Siryaporn E, Hixson DC, Akerley W. Survival of docetaxel-resistant prostate cancer cells in vitro depends on phenotype alterations and continuity of drug exposure. Cell Mol Life Sci 2002;59:1198–211.
7. Patterson SG, Wei S, Chen X, Sallman DA, Gilvary DL, Zhong B, et al. Novel role of Stat1 in the development of docetaxel resistance in prostate tumor cells. Oncogene 2006;25:6113–22.
8. Hara T, Ushio K, Nishiwaki M, Kouno J, Araki H, Hikichi Y, et al. A mutation in beta-tubulin and a sustained dependence on androgen receptor signalling in a newly established docetaxel-resistant prostate cancer cell line. Cell Biol Int 2010;34:177–84.
9. Carter PJ, Senter PD. Antibody-drug conjugates for cancer therapy. Cancer J 2008;14:154–69.
10. Polakis P. Arming antibodies for cancer therapy. Curr Opin Pharmacol 2005;5:382–7.
11. Younes A, Bartlett NL, Leonard JP, Kennedy DA, Lynch CM, Sievers EL, et al. Brentuximab vedotin (SGN-35) for relapsed CD30-positive lymphomas. N Engl J Med 2010;363:1812–21.
12. Reichert JM, Valge-Archer VE. Development trends for monoclonal antibody cancer therapeutics. Nat Rev Drug Discov 2007;6: 349–56.
13. Alley SC, Okeley NM, Senter PD. Antibody-drug conjugates: targeted drug delivery for cancer. Curr Opin Chem Biol 2010;14:529–37.
14. Gerber HP, Senter PD, Grewal IS. Antibody drug-conjugates targeting the tumor vasculature: Current and future developments. MAbs 2009;1:247–53.
15. Junutula JR, Raab H, Clark S, Bhakta S, Leipold DD, Weir S, et al. Site-specific conjugation of a cytotoxic drug to an antibody improves the therapeutic index. Nat Biotechnol 2008;26:925–32.
16. Krop IE, Beeram M, Modi S, Jones SF, Holden SN, Yu W, et al. Phase I study of trastuzumab-DM1, an HER2 antibody-drug conjugate, given every 3 weeks to patients with HER2-positive metastatic breast cancer. J Clin Oncol 2010;28:2698–704.
17. Israeli RS, Powell CT, Corr JG, Fair WR, Heston WD. Expression of the prostate-specific membrane antigen. Cancer Res 1994;54: 1807–11.
18. Davis MI, Bennett MJ, Thomas LM, Bjorkman PJ. Crystal structure of prostate-specific membrane antigen, a tumor marker and peptidase. Proc Natl Acad Sci U S A 2005;102:5981–6.
19. Olson WC, Heston WDW, Rajasekaran AK. Clinical trials of cancer therapies targeting prostate-specific membrane antigen. Reviews on Recent Clinical Trials 2007;2:182–90.
20. Wright GL Jr., Grob BM, Haley C, Grossman K, Newhall K, Petrylak D, et al. Upregulation of prostate-specific membrane antigen after androgen-deprivation therapy. Urology 1996;48:326–34.
21. Bostwick DG, Pacelli A, Blute M, Roche P, Murphy GP. Prostate specific membrane antigen expression in prostatic intraepithelial neoplasia and adenocarcinoma: a study of 184 cases. Cancer 1998; 82:2256–61.
22. Sweat SD, Pacelli A, Murphy GP, Bostwick DG. Prostate-specific membrane antigen expression is greatest in prostate adenocarcinoma and lymph node metastases. Urology 1998;52:637–40.
23. Chang SS, Gaudin PB, Reuter VE, O'Keefe DS, Bacich DJ, Heston WD. Prostate-Specific Membrane Antigen: Much More Than a Prostate Cancer Marker. Mol Urol 1999;3:313–20.
24. Chang SS, Reuter VE, Heston WD, Bander NH, Grauer LS, Gaudin PB. Five different anti-prostate-specific membrane antigen (PSMA) antibodies confirm PSMA expression in tumor-associated neovasculature. Cancer Res 1999;59:3192–8.
25. Troyer JK, Beckett ML, Wright GLJ. Detection and characterization of the prostate-specific membrane antigen (PSMA) in tissue extracts and body fluids. Int J Cancer 1995;62:552–8.
26. Rajasekaran SA, Anilkumar G, Oshima E, Bowie JU, Liu H, Heston W, et al. A novel cytoplasmic tail MXXXL motif mediates the internalization of prostate-specific membrane antigen. Mol Biol Cell 2003;14: 4835–45.
27. Liu H, Rajasekaran AK, Moy P, Xia Y, Kim S, Navarro V, et al. Constitutive and antibody-induced internalization of prostate-specific membrane antigen. Cancer Res 1998;58:4055–60.
28. Vaishampayan U, Glode M, Du W, Kraft A, Hudes G, Wright J, et al. Phase II study of dolastatin-10 in patients with hormone-refractory metastatic prostate adenocarcinoma. Clin Cancer Res 2000;6: 4205–8.
29. Madden T, Tran HT, Beck D, Huie R, Newman RA, Pusztai L, et al. Novel marine-derived anticancer agents: a phase I clinical, pharmacological, and pharmacodynamic study of dolastatin 10 (NSC 376128) in patients with advanced solid tumors. Clin Cancer Res 2000;6: 1293–301.
30. Oflazoglu E, Kissler KM, Sievers EL, Grewal IS, Gerber HP. Combination of the anti-CD30-auristatin-E antibody-drug conjugate (SGN-35) with chemotherapy improves antitumour activity in Hodgkin lymphoma. Br J Haematol 2008;142:69–73.
31. Ma D, Hopf C, Malewicz AD, Donovan GD, Senter PD, Goeckeler WF, et al. Potent antitumor activity of an auristatin-conjugated, fully human monoclonal antibody to prostate-specific membrane antigen. Clin Cancer Res 2006;12:2591–6.
32. Petrylak D, Kantoff PW, Rotshteyn Y, Israel RJ, Olson WC, Ramakrishna T, et al. Prostate-specific membrane antigen antibody-drug conjugate (PSMA ADC): A phase 1 trial in taxane refractory prostate cancer. 2011ASCO Genitourinary Cancers Symposium, Abstract #72560, Orlando, FL, 2011.
33. Ghosh A, Heston WD. Effect of carbohydrate moieties on the folate hydrolysis activity of the prostate specific membrane antigen. Prostate 2003;57:140–51.
34. Ghosh A, Wang X, Klein E, Heston WD. Novel role of prostate-specific membrane antigen in suppressing prostate cancer invasiveness. Cancer Res 2005;65:727–31.
35. Heston WD. Characterization and glutamyl preferring carboxypeptidase function of prostate specific membrane antigen: a novel folate hydrolase. Urology 1997;49:104–12.
36. Carter RE, Feldman AR, Coyle JT. Prostate-specific membrane antigen is a hydrolase with substrate and pharmacologic characteristics of a neuropeptidase. Proc Natl Acad Sci U S A 1996;93:749–53.
37. Foss CA, Mease RC, Fan H, Wang Y, Ravert HT, Dannals RF, et al. Radiolabeled small-molecule ligands for prostate-specific membrane antigen: in vivo imaging in experimental models of prostate cancer. Clin Cancer Res 2005;11:4022–8.
38. Schulke N, Varlamova OA, Donovan GP, Ma D, Gardner JP, Morrissey DM, et al. The homodimer of prostate-specific membrane antigen is a functional target for cancer therapy. Proc Natl Acad Sci U S A 2003;100:12590–5.

39. Hari M, Loganzo F, Annable T, Tan X, Musto S, Morilla DB, et al. Paclitaxel-resistant cells have a mutation in the paclitaxel-binding region of beta-tubulin (Asp26Glu) and less stable microtubules. Mol Cancer Ther 2006;5:270–8.
40. Henry MD, Wen S, Silva MD, Chandra S, Milton M, Worland PJ. A prostate-specific membrane antigen-targeted monoclonal antibody-chemotherapeutic conjugate designed for the treatment of prostate cancer. Cancer Res 2004;64:7995–8001.
41. Moffett S, Melancon D, DeCrescenzo G, St-Pierre C, Deschenes F, Saragovi HU, et al. Preparation and characterization of new anti-PSMA monoclonal antibodies with potential clinical use. Hybridoma (Larchmt)2007;26:363–72.
42. Barinka C, Sacha P, Sklenar J, Man P, Bezouska K, Slusher BS, et al. Identification of the N-glycosylation sites on glutamate carboxypeptidase II necessary for proteolytic activity. Protein Sci 2004;13:1627–35.
43. Minner S, Wittmer C, Graefen M, Salomon G, Steuber T, Haese A, et al. High level PSMA expression is associated with early psa recurrence in surgically treated prostate cancer. Prostate 2010;71:281–8.
44. Tannock IF, De Wit R, Berry WR, Horti J, Pluzanska A, Chi KN, et al. Docetaxel plus prednisone or mitoxantrone plus prednisone for advanced prostate cancer. N Engl J Med 2004;351:1502–12.
45. Lee JT Jr., Steelman LS, McCubrey JA. Phosphatidylinositol 3′-kinase activation leads to multidrug resistance protein-1 expression and subsequent chemoresistance in advanced prostate cancer cells. Cancer Res 2004;64:8397–404.
46. O'Brien C, Cavet G, Pandita A, Hu X, Haydu L, Mohan S, et al. Functional genomics identifies ABCC3 as a mediator of taxane resistance in HER2-amplified breast cancer. Cancer Res 2008;68:5380–9.
47. Hopper-Borge E, Chen ZS, Shchaveleva I, Belinsky MG, Kruh GD. Analysis of the drug resistance profile of multidrug resistance protein 7 (ABCC10): resistance to docetaxel. Cancer Res 2004;64:4927–30.
48. Hill BT, Whelan RD, Shellard SA, McClean S, Hosking LK. Differential cytotoxic effects of docetaxel in a range of mammalian tumor cell lines and certain drug resistant sublines *in vitro*. Invest New Drugs 1994;12:169–82.
49. Netti PA, Hamberg LM, Babich JW, Kierstead D, Graham W, Hunter GJ, et al. Enhancement of fluid filtration across tumor vessels: implication for delivery of macromolecules. Proc Natl Acad Sci U S A 1999;96:3137–42.
50. Kuroda K, Liu H, Kim S, Guo M, Navarro V, Bander NH. Docetaxel down-regulates the expression of androgen receptor and prostate-specific antigen but not prostate-specific membrane antigen in prostate cancer cell lines: implications for PSA surrogacy. Prostate 2009;69:1579–85.